PHYSICAL REVIEW B VOLUME 23, NUMBER 11 1 JUNE 1981

Temperature dependence of the Faraday rotation of lead- and bismuth-substituted gadolinium iron garnet films at 633 nm

P. Hansen, H. Heitmann, and K. Witter
Philips GmbH Forschungslaboratorium Hamburg, D-2000 Hamburg 54, Germany
(Received 5 December 1980)

The Faraday rotation of epitaxial garnet films of composition $Gd_{3-x}Pb_xFe_5O_{12}$ with $x \leq 0.36$ and $Gd_{3-x}Bi_xFe_{5-y}Ga_yO_{12}$ with $0 \leq x, y \leq 1$ has been investigated in the temperature range $4.2\ \text{K} \leq T \leq T_C$ at $\lambda = 633$ nm. The experimental data can be described in terms of the corresponding sublattice magnetizations which were deduced from the fit of the molecular-field theory to the measured saturation magnetizations. The tetrahedral and octahedral magneto-optical coefficients turned out to be temperature independent. The negative tetrahedral coefficient is increased in magnitude, and the octahedral coefficient exhibited a strong reduction with increasing Pb and Bi content. The contribution to the Faraday rotation per formula unit $\Delta\theta_F/x$ for Pb and Bi at $T = 295$ K was found to be -7700 and -18000 deg cm^{-1}, respectively. The measured wavelength dependence of the Faraday rotation and the Faraday ellipticity showed similar characteristics for both systems, indicating that the basic mechanisms causing the magneto-optical behavior via the increased superexchange are of the same type.

I. INTRODUCTION

Bismuth and lead are known to induce large magneto-optical effects in the rare-earth iron garnets. This has led to a variety of fundamental investigations[1–5] and the development of technical applications.[6,7] Many investigators have treated the Faraday rotation, Kerr rotation, and optical absorption concerning the compositional and wavelength dependence of bismuth-substituted garnets while the influence of lead on these properties has been discussed much less intensively. Moreover, there has been made no attempt to study the temperature dependence at $\lambda = 633$ nm. This HeNe laser wavelength, however, being far from the center of magneto-optical transitions, in the range of low optical absorption, appears to be very interesting from the experimental point of view and in particular for devices based on light modulation components. This situation is similar for other garnet compositions where only a few authors dealt with the temperature behavior at larger wavelengths.[8–15] However, this feature is quite important for the understanding of the influence of these ions on the relationship between the sublattice magnetizations and the sublattice rotations, i.e., on the magneto-optical coefficients which reflect the enhancement of the optical iron transitions by the Pb and Bi ions. In addition, the knowledge of these coefficients offers the possibility to predict the Faraday rotation for arbitrary substitutions and temperatures and to determine special features such as its compensation temperature.

The aim of this work, therefore, is the study of the temperature and compositional dependence of the Faraday rotation of lead- and bismuth-substituted gadolinium iron garnets at $\lambda = 633$ nm. Two series of epitaxial films of composition $Gd_{3-x}Pb_xFe_5O_{12}$ and $Gd_{3-x}Bi_xFe_{5-y}Ga_yO_{12}$ were investigated. In Sec. II the calculation of the sublattice magnetizations from the fit of the molecular-field theory to the measured data of the saturation magnetization is presented. In Sec. III the Faraday rotation is described in terms of the sublattice magnetizations and the magneto-optical coefficients are determined as a function of the Pb and Bi content. In Sec. IV the results are interpreted and the different magneto-optical behavior of these ions is discussed.

II. MAGNETIZATION

A. Film characterization

The garnet films investigated were grown by liquid phase epitaxy onto (111) oriented magnesium-, calcium-, and zirconium-substituted gadolinium gallium garnet substrates.[16] For the lead-substituted films a bismuth-free PbO-B_2O_3 based flux was used and for the bismuth-substituted films a Bi_2O_3-PbO-B_2O_3 based flux.[17] The growth temperatures ranged between 1000 and 1200 K and the thickness of the films between 2 and 7 μm. The chemical analysis data of selected film compositions used for the temperature-dependent measurements are compiled in Table I. The gallium content of the bismuth films on the one hand was necessary to account for the mismatch conditions concerning the available substrates and on the other hand made it possible to study the influence of diamagnetic tetrahedral substi-

TABLE I. Chemical analysis data and the concentration on tetrahedral (d), octahedral (a), and dodecahedral (c) sites used to fit the saturation magnetization data.

Composition	Sample No.	Substitution x	Substitution y	Impurity Pb	Impurity Pt	Accuracy	Molecular-field theory x	Molecular-field theory y_a	Molecular-field theory y_d
$Y_3Fe_5O_{12}$	1	· · ·	· · ·	<0.01	0.006		0	0	0
$Gd_3Fe_5O_{12}$[a]	2	· · ·	· · ·	0.01	0.01		0.01	0.01	0
$Gd_{3-x}Pb_xFe_5O_{12}$	3	0.06	· · ·	· · ·	0.03	Pb: ±0.01	0.06[b]	0.07[b]	0
	4	0.18	· · ·	· · ·	0.04	Pt: ±0.005	0.17[b]	0.11[b]	0
	5	0.36	· · ·	· · ·	0.05		0.37[b]	0.14[b]	0
	6	0.15	0.20	0.02	0.02	Ga: ±0.01	0.16	0.02	0.21
	7	0.58	0.16	0.04	0.04	Al: ±0.01	0.64	0.05	0.16
$Gd_{3-x}Bi_xFe_{5-y}Ga_yO_{12}$	8	0.62	0.36	0.04	0.04	Bi: ±0.03	0.60	0.05	0.40
	9	0.62	0.83[c]	0.04	0.04	Pt: ±0.01	0.62	0.10	0.81
	10	1.00	0.31	0.06	0.05	Pb: ±0.015	1.06	0.06	0.30

[a]For the θ_F measurements a 100-μm-thick platelet with the same impurity content was used.
[b]x and y_a represent the concentrations calculated according to case (vi) in Table II for a and c sites, respectively.
[c]This sample contains 0.29 aluminum.

tutions on the magneto-optical effects.

The saturation magnetization M_s was measured with a vibrating sample magnetometer and the Faraday rotation θ_F with an optical hysteresigraph in the temperature range 4.2 K $\leq T \leq T_C$. Both properties were obtained by extrapolation to zero field ($H \leq 1.6 \times 10^6$ A/m for M_s and $H \leq 1.3 \times 10^6$ A/m for θ_F).

B. Sublattice magnetizations

The temperature dependence of the Faraday rotation is expected to be governed by that of the sublattice magnetizations.[8] The latter can be deduced from the fit of the molecular-field theory to the measured saturation magnetization M_s.[18,19] The sublattice magnetizations $M_i(T,z)$ as a function of temperature T and concentration $z=f(x,y)$ can be calculated from the expressions

$$M_i(T,z)=M_i(0,z)B_{S_i}\left(\frac{g_i\mu_B S_i}{kT}\sum_j N_{ij}(z)M_j(T,z)\right),$$
$$M_s(T,z)=|M_c(T,z)+M_a(T,z)-M_d(T,z)|, \quad (1)$$

where S_i, g_i, $N_{ij}(z)$, and $B_{S_i}(u_{ij})$ are the spin quantum numbers on the ith sublattice, the spectroscopic splitting factors, the molecular-field constants, and the Brillouin functions, respectively. μ_B is the Bohr magneton and k the Boltzmann constant. j runs over the three sublattices a, d, and c. The concentration dependence of $M_i(0,z)$ and $N_{ij}(z)$ for diamagnetically diluted gadolinium iron garnets has been determined empirically.[19] Using the set of equations given in Ref. 19, except for the exchange constant $N_{ad}(z)$ which has been slightly modified according to the relation

$$N_{ad}(z)=96.9(1+ax-0.125y_a-0.127y_d), \quad (2)$$
$$y=y_a+y_d,$$

a good fit of the experimental saturation magnetization data can be achieved. The small reduction of $N_{ad}(0)$ in comparison with that of Ref. 19 is due to the sightly lower Curie temperature T_C of our "pure" gadolinium iron garnet. The additional term ax accounts for the increase of T_C with the lead ($a=0.049$) and the bismuth ($a=0.035$) content. For $x_{Bi}=1$ the rise of T_C is about 38 K which is in good agreement with the value reported for $Y_{3-x}Bi_xFe_5O_{12}$.[20] For the calculations $g_a=g_d=g_c=2$, $S_a=S_d=\frac{5}{2}$, and $S_c=\frac{7}{2}$ have been used.

1. *Lead-substituted films*

The variation of the compensation temperature T_{comp} and the saturation magnetization with the lead content is shown in Figs. 1 and 2. It turns out that the decrease of T_{comp} is much stronger than expected for a pure diamagnetic dodecahedral substitution (dashed line in Fig. 1). Since T_{comp} is very sensitive with respect to any change in the occupation of the different lattice sites this indicates that no pure self-compensation Pb^{2+}-Pb^{4+} on dodecahedral sites occurred and that the octahedral sites must be involved

TABLE II. Calculated lattice mismatch Δa and compensation temperature T_{comp} for different possible distributions of the charge compensation ions for sample 5 (see Table I). The experimental data of Δa and T_{comp} are $(2.4 \pm 0.2) \times 10^{-3}$ nm and (223 ± 1) K, respectively.

	Distribution		Lattice mismatch Δa	T_{comp}
	a	c	(10^{-3} nm)	(K)
i	Pt^{4+}	Pb^{2+}, Pb^{4+}	2.6	241
ii	Pb^{4+}, Pt^{4+}	Pb^{2+}	5.4	228
iii	Fe^{4+}, Pt^{4+}	Pb^{2+}	4.9	223
iv	Fe^{2+}, Pt^{4+}	Pb^{4+}	−1.0	223
v	Pb^{4+}, Pt^{4+}	Fe^{2+}	0.4	184
vi	Pb^{4+}, Pt^{4+}	$Pb^{2+}, Pb^{4+}, Fe^{2+}$	2.4	223

to some extent.[3] There are different possibilities to maintain the charge compensation. These are summarized in Table II together with the calculated T_{comp} values for sample 5 exhibiting the highest lead content. It turned out that different configurations can account for the observed T_{comp} value. Therefore, in addition the measured mismatch $\Delta a = 0.55 \Delta a^{\perp}$ with reference to the lattice constant of pure gadolinium gallium garnet was considered and compared with the calculated mismatch[21,22] also given in Table II. The presence of boron and oxygen vacancies which cannot be excluded have not been taken into account. $\Delta a^{\perp}$ is the directly measured lattice mismatch perpendicular to the film plane. The measured Δa increases linearly with the lead content up to $(2.4 \pm 0.2) \times 10^{-3}$ nm (sample 5). From Table II it is obvious that the more complicated configuration (vi) where roughly half of the lead is in the divalent state meets both requirements within the limits of experimental error. The calculated concentration dependence of T_{comp}

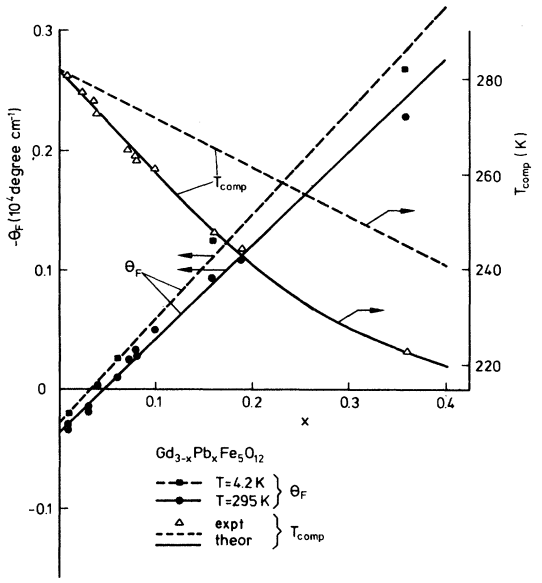

FIG. 1. Concentration dependence of the Faraday rotation θ_F at $\lambda = 633$ nm and the compensation temperature T_{comp} of gadolinium-lead iron garnet films. The theoretical curves for T_{comp} are based on different distributions on octahedral and dodecahedral sites of the ions involved (see text).

and the temperature dependence of $4\pi M_s$ based on this configuration are represented by the solid lines in Figs. 1 and 2 which reproduce the experimental data quite well. The concentrations needed for these fits are listed in Table I and the comparison with the chemical analysis data shows that for all samples the calculated and measured concentrations are in agreement within the limits of error. The measured magnetic data are summarized in Table III.

TABLE III. Measured magnetic and magneto-optical (at $\lambda = 633$ nm) data of the investigated garnet films.

Composition	Sample No.	$4\pi M_s$ (mT) $T = 4.2$ K	$4\pi M_s$ (mT) $T = 295$ K	θ_F (deg cm^{-1}) $T = 4.2$ K	θ_F (deg cm^{-1}) $T = 295$ K	T_{comp} (K)	T_C (K)
$Y_3Fe_5O_{12}$	1	247	180	235	760	. . .	559
$Gd_3Fe_5O_{12}$	2	771	7	200[a]	345[a]	283	562
	3	736	15	−260	− 93	259	561
$Gd_{3-x}Pb_xFe_5O_{12}$	4	689	24	−1310	−974	248	561
	5	613	35	−2690	−2310	223	560
	6	762	2	−3640	−2920	302	538
	7	577	29	−12400	−10500	226	556
$Gd_{3-x}Bi_xFe_{5-y}Ga_yO_{12}$	8	648	4	−11950	−10100	283	527
	9	729	30	−9000	−7200	. . .	472
	10	464	36	−22100	−18900	197	551

[a]Measured on a 100-μm-thick platelet.

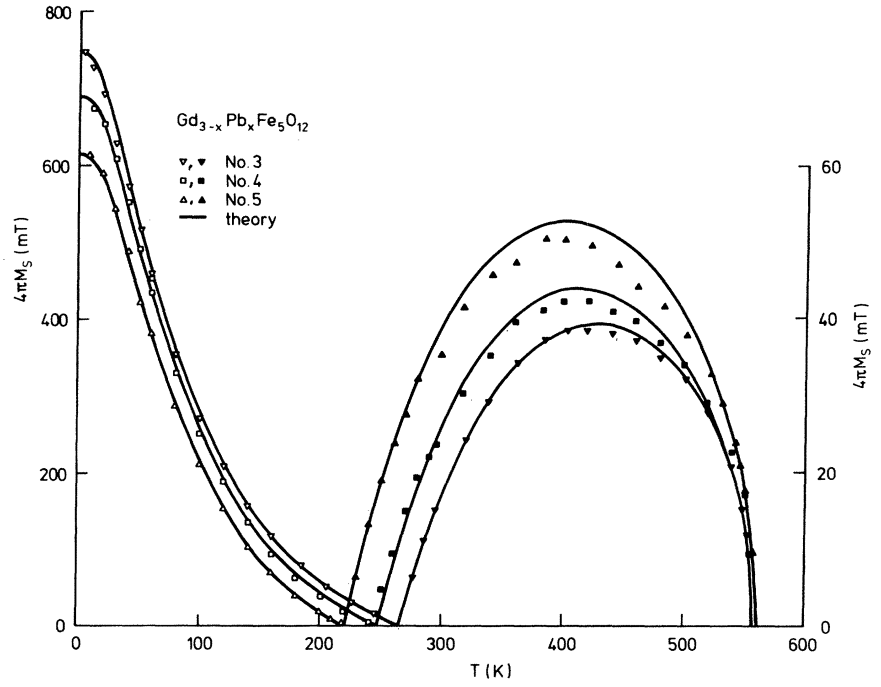

FIG. 2. Temperature dependence of the saturation magnetization $4\pi M_s$ of gadolinium-lead iron garnet films. The theoretical curves (solid lines) are calculated from the molecular-field theory [Eqs. (1)]. The data for $T < T_{comp}$ (open symbols) apply to the left scale and those for $T > T_{comp}$ (solid symbols) to the right scale.

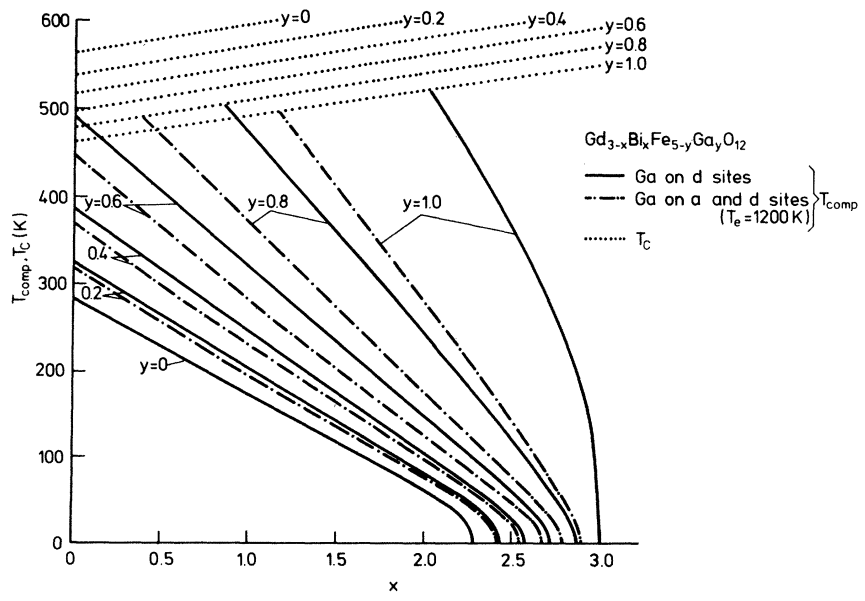

FIG. 3. Calculated concentration dependence of the Curie temperature T_C (dotted line) and the compensation temperature T_{comp} of gadolinium-bismuth iron-gallium garnet films. The solid lines represent the case of a pure tetrahedral occupation of the gallium ions and the dashed-dotted lines represent the case of a distribution over octahedral and tetrahedral sites applying to an equilibrium temperature $T_e = 1200$ K (see Fig. 4).

2. *Bismuth-substituted films*

For bismuth-substituted gadolinium iron-gallium garnets the magnetic properties solely are affected by the diamagnetic dilution on dodecahedral sites and the change of the iron exchange presumably induced by their large ionic radius of the Bi^{3+} ions. These influences cause a decrease of T_{comp} and a rise of T_C with increasing Bi content which has been calculated from Eq. (1) for different gallium concentrations. The results are displayed in Fig. 3. Since a small fraction of the gallium ions enters octahedral sites T_{comp} significantly depends on the gallium distribution[23] which is determined by the thermal history.[24,25] These dependences can be calculated on the basis of a gallium distribution being present in bulk crystals of composition $Y_3Fe_{5-y}Ga_yO_{12}$ induced by annealing treatments[25] and they are in agreement with the measured data. For temperatures corresponding to the equilibrium temperatures T_e of the investigated films the fraction of gallium ions on octahedral sites as a function of the total gallium content is shown in Fig. 4. With these data a good fit of the saturation magnetization of all bismuth-substituted samples was achieved, as is shown in Figs. 5(a) and 5(b). The ion concentrations deduced from these fits are given in Table I. They are in good agreement with the chemical analysis data except for sample 8 were a slightly higher tetrahedral gallium content was needed to reproduce the M_s curve. The measured magnetic data are listed in Table III.

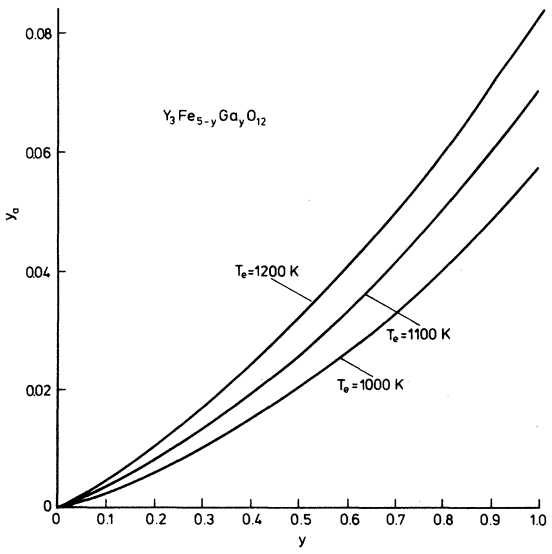

FIG. 4. Fraction of octahedral gallium ions vs total gallium content for different equilibrium temperatures.

III. FARADAY ROTATION

A. Temperature dependence of $Y_3Fe_5O_{12}$ and $Gd_3Fe_5O_{12}$

The variation of the Faraday rotation θ_F with temperature and concentration for a three-sublattice rare-earth iron garnet can be written[8]

$$\theta_F(T,z) = A(z)M_a(T,z) + D(z)M_d(T,z) + C(z)M_c(T,z) \ , \tag{3}$$

where $z = f(x,y)$ formally represents the concentration dependence. The magneto-optical coefficients are composed of an electric and a magnetic dipole transition coefficient

$$A = -A_e - A_m \ , \quad D = D_e + D_m \ , \quad C = -C_e - C_m \ . \tag{4}$$

The magnetic dipole transition coefficients are given by $\pi \bar{n} e g_i / mc^2$ where $\bar{n}$ is the mean refractive index. Since $\bar{n}$ exhibits a weak dependence on composition and $g_a = g_d = g_c = 2$ for diamagnetically substituted gadolinium iron garnets the magnetic dipole transition coefficients can approximately be regarded as constants. When the sublattice moments are expressed in Bohr magnetons per two formula units these coefficients have the value

$$A_m = D_m = C_m = 9.57 \mu_B^{-1} \ \text{deg cm}^{-1} \ , \tag{5}$$

where $\bar{n} = 2.3$ for $Y_3Fe_5O_{12}$ at $\lambda = 633$ nm has been used.[26,27] The electric dipole transition coefficients then can be deduced from the fit to the measured temperature variation of θ_F. The theory predicts temperature-independent coefficients[8] and this has been confirmed for several rare-earth iron garnets at $\lambda = 1150$ nm.[8,12] However, there are other investigators reporting a strong temperature dependence of these coefficients.[9,15]

The results of our θ_F measurements for $Y_3Fe_5O_{12}$ and $Gd_3Fe_5O_{12}$ at $\lambda = 633$ nm are shown in Fig. 6. For $Y_3Fe_5O_{12}$ an excellent fit was achieved for the whole temperature range with temperature-independent coefficients (solid line). The sublattice magnetizations were calculated from Eqs. (1) based on the molecular-field constants $N_{aa} = -67.7$, $N_{dd} = -30.4$, and $N_{ad} = 98.0$, expressed in mol cm^{-3}. They are in good agreement with the measured sublattice magnetizations by the NMR technique.[25] This description of θ_F with constant coefficients is in accordance with another representation of the experimental data. Plotting M_a/θ_F^0 as a function of M_d/θ_F^0 from Eq. (3) a straight line is expected. $\theta_F^0 = \theta_F - CM_c$ denotes the rotation of the iron sublattices. In Fig. 7 this relationship is shown and it turns out

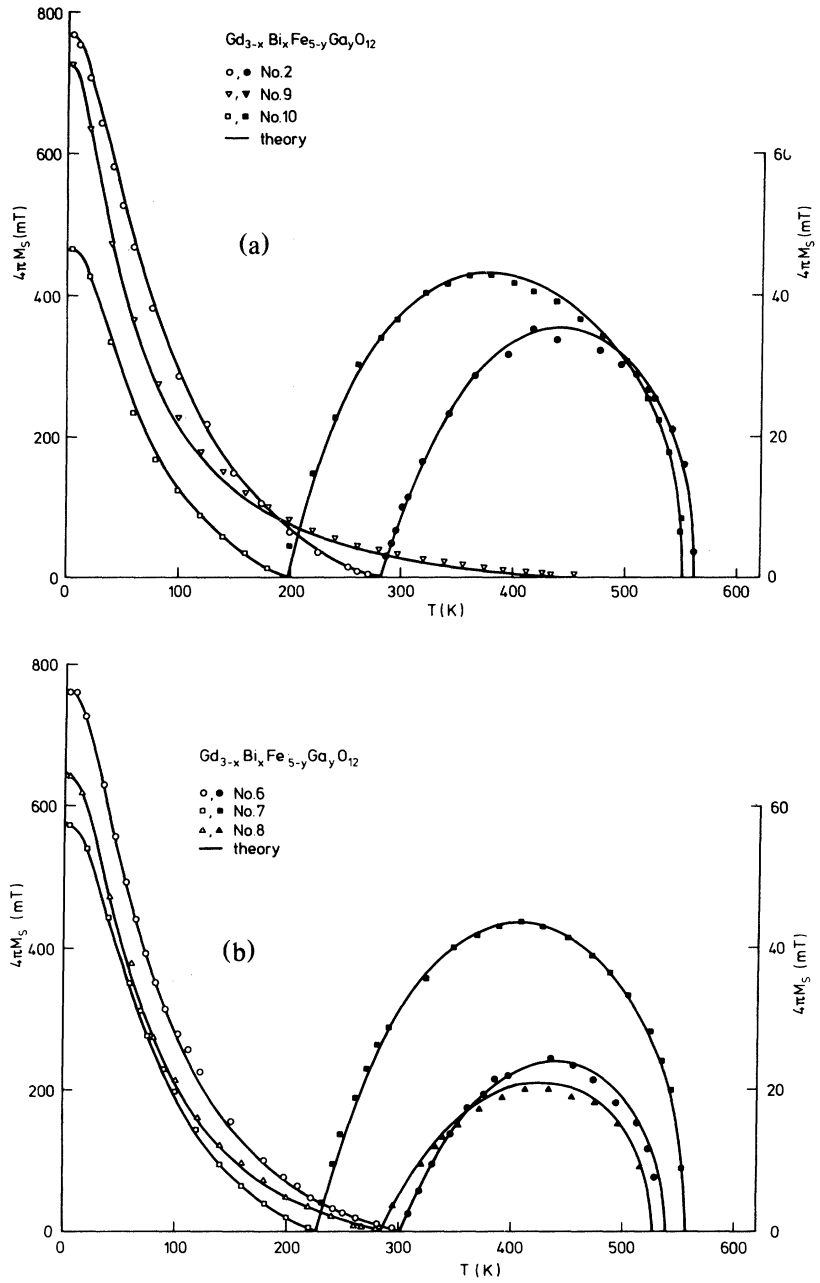

FIG. 5. (a),(b) Temperature dependence of the saturation magnetization $4\pi M_s$ of gadolinium-bismuth iron-gallium garnet films. The theoretical curves (solid lines) are calculated from the molecular-field theory [Eqs. (1)] based on a gallium distribution given in Fig. 4. The data for $T < T_{comp}$ (open symbols) apply to the left scale and those for $T > T_{comp}$ (solid symbols) to the right scale.

that it is exactly linear. For $Gd_3Fe_5O_{12}$ the agreement between theory and experiment is less satisfactory (dashed line in Fig. 6). In this case an improvement was obtained assuming A and D to be constants but C to be temperature dependent (solid line). This dependence of $C_e = -C - 9.57$ on T is displayed in Fig. 8. The constant C_e value used in the fit with constant coefficients is presented in Fig. 8 by the dashed line. This approach with a temperature-dependent dodecahedral coefficient confirms the reported data on a temperature dependence of C_e in rare-earth iron garnets.[15] For the investigation of the

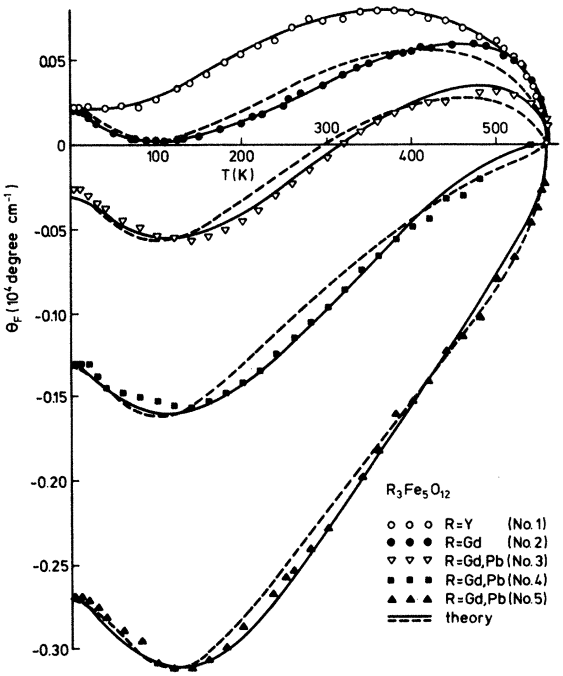

FIG. 6. Temperature dependence of the Faraday rotation of yttrium iron garnet and gadolinium-lead iron garnet films at $\lambda = 633$ nm. The theoretical curves have been calculated from Eq. (3) for temperature independent coefficients at *a* (octahedral), *d* (tetrahedral), and *c* (dodecahedral) sites (dashed lines) and temperature independent coefficients at *a* and *d* sites but a temperature dependent coefficient at the *c* site (solid lines).

lead- and bismuth-substituted garnets a comparison of the following two cases, (I) A,D,C are independent of T, and (II) A,D are independent of T but C depends on T, will be made and the influence on the deduced coefficients will be discussed.

B. Temperature dependence of θ_F and the magneto-optical coefficients of lead- and bismuth-substituted garnet films

1. Lead-substituted films

The substitution of lead gives rise to a large increase of the optical absorption α,[3] the Faraday rotation θ_F,[28] and the Faraday ellipticity $\epsilon_F = \tan\psi_F$, which can be attributed to the increased superexchange causing the raised Curie temperatures. The variation of θ_F with the Pb content for the films of composition $Gd_{3-x}Pb_xFe_5O_{12}$ is shown in Fig. 1 for two temperatures. The contribution $\Delta\theta_F(x) = \theta_F(x) - \theta_F(0)$ per formula unit $\Delta\theta_F/x$ was obtained to be about -7700 deg cm^{-1} for both temperatures. From the linear increase of the optical absorption and the Faraday ellipticity at $T = 295$ K, $\Delta\alpha/x$ was found to be 1280 cm^{-1} and $\Delta\psi_F/x$ roughly equals $\Delta\theta_F/x$ at $\lambda = 633$ nm. For higher lead contents a deviation from linearity may occur owing to a change in the distribution of the charge compensating ions. The temperature dependence of θ_F for three Pb substitutions is displayed in Fig. 6. The minimum of θ_F at

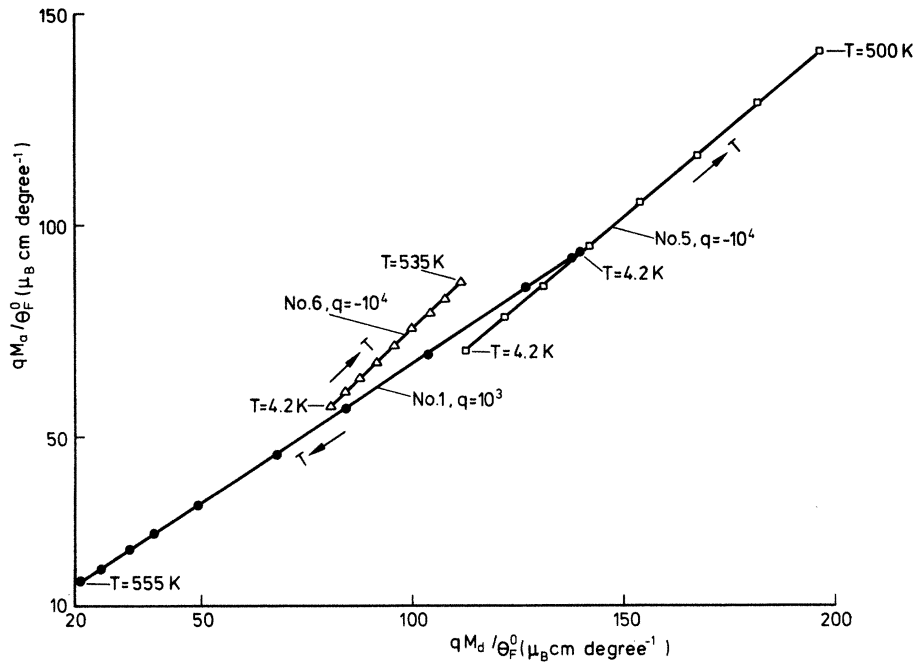

FIG. 7. Variation of M_a/θ_F^0 as a function of M_d/θ_F^0 for three films of composition $Y_3Fe_5O_{12}$ (sample 1), $(Gd,Pb)_3Fe_5O_{12}$ (sample 5), and $(Gd,Bi)_3(Fe,Ga)_5O_{12}$ (sample 6) where θ_F^0 denotes the rotation of the iron sublattices. The linear relationship indicates that the magneto-optical coefficients involved are temperature-independent quantities. q is a scaling factor.

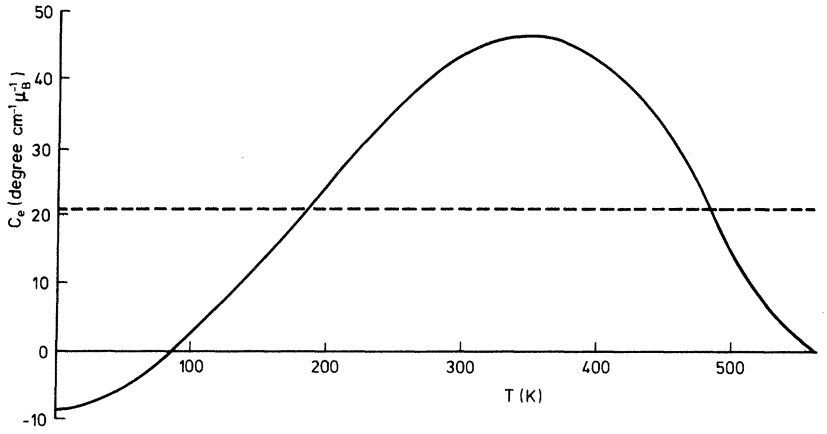

FIG. 8. Electric dipole transition coefficient C_e deduced from the fit of the Faraday rotation of gadolinium iron garnet (see text).

about $T=100$ K of pure $Gd_3Fe_5O_{12}$ which has to be assigned to the contribution of the dodecahedral sites obviously is enhanced by the lead. Thus all sites are expected to be affected by the Pb ions. Using case (I) (dashed lines) the essential features of the temperature variation can be described but there remain some deviations. With case (II) (solid lines), however, a good fit of the measured data was achieved assuming $C_e(T)$ to depend on x as

$$C_e(T,x)=C_0(1+3.26x)f(T) \quad . \tag{6}$$

C_0 and $f(T)$ determine $C_e(T,0)\equiv C_e(T)$ for pure $Gd_3Fe_5O_{12}$ and can be extracted from Fig. 8.

The contribution $\theta_F^0=\theta_F-CM_c$ of the iron sublattices to the rotation is described in both models by temperature independent constants A and D and thus for the plot of M_a/θ_F^0 vs M_d/θ_F^0 again a linear relationship is expected. This indeed is fulfilled for the measured Pb substitutions and is shown in Fig. 7 for sample 5 with the highest Pb content.

The concentration dependences of the deduced magneto-optical coefficients are represented in Fig. 9 for both cases. $C(T,x)$ in case (II) is plotted at $T=185$ K where it is equal to the C value in case (I) at $x=0$ (see Fig. 8). For the tetrahedral and dodecahedral sites the same tendency occurred while the octahedral coefficients exhibited a different behavior for these two cases. This situation will be discussed in Sec. IV.

The electrical dipole coefficients for both cases are compiled in Table IV.

2. *Bismuth-substituted films*

The variation of θ_F with the bismuth content is substantially larger than for lead although the physical origin is based on similar mechanisms. The bismuth enhances the intensities of the iron pair

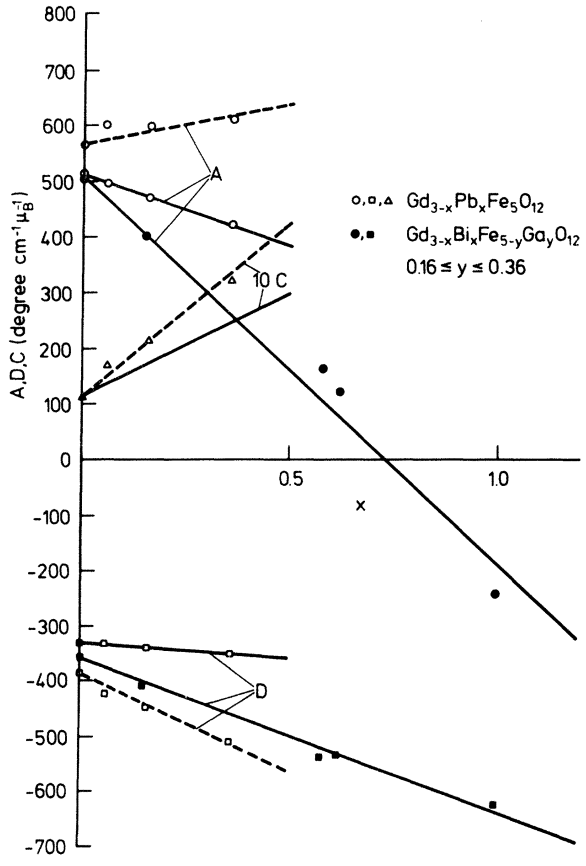

FIG. 9. Concentration dependence of the magneto-optical coefficients of lead- and bismuth-substituted gadolinium iron (-gallium) garnet films for temperature-independent coefficients (dashed lines) and for the case that A and D are temperature independent but C depends on temperature (solid lines). For case (II) $C(T,x)$ is presented for $T=185$ K and for both cases the dodecahedral coefficients are scaled up by a factor of 10.

TABLE IV. Electric dipole transition coefficients for two adjustments of the theory to the experimental data at $\lambda = 633$ nm. In case (I) C_e has been assumed to be temperature independent and in case (II) C_e was temperature dependent and therefore is omitted in this table (see Fig. 8). A_e and D_e were assumed to be temperature independent in both cases. A_e, D_e, and C_e are related to the coefficients A, D, and C in Eq. (3) by: $A_e = -A - 9.57$, $D_e = D + 9.57$, $C_e = -C - 9.57$.

Composition	Sample No.	A_e (μ_B^{-1} deg cm^{-1}) I	A_e (μ_B^{-1} deg cm^{-1}) II	D_e (μ_B^{-1} deg cm^{-1}) I	D_e (μ_B^{-1} deg cm^{-1}) II	C_e (μ_B^{-1} deg cm^{-1}) I
$Y_3Fe_5O_{12}$	1	−520.0	. . .	−323.6	. . .	. . .
$Gd_3Fe_5O_{12}$	2	−573.7	−520.0	−375.9	−323.6	−20.8
	3	−612.2	−505.9	−414.0	−320.4	−27.1
$Gd_{3-x}Pb_xFe_5O_{12}$	4	−606.2	−482.2	−440.8	−330.8	−31.2
	5	−620.7	−430.5	−502.5	−342.0	−42.6
	6	−636.4	−413.1	−574.8	−397.7	−19.5
	7	−432.2	−174.8	−749.6	−529.0	−22.9
$Gd_{3-x}Bi_xFe_{5-y}Ga_yO_{12}$	8	−25.1	−127.8	−459.5	−526.1	−17.3
	9	−2459.7	−2636.8	−2527.9	−2676.1	−13.2
	10	+296.4	+237.0	−581.2	−636.3	−13.2

transitions as a result of the increased superexchange[29] which also caused the increased Curie temperatures. The concentration dependence of θ_F of the investigated films of composition $Gd_{3-x}Bi_xFe_{5-y}Ga_yO_{12}$ is given in Fig. 10 for two temperatures. The increase per formula unit $\Delta\theta_F/x$ turns out to be $-18\,000$ deg cm^{-1} at $T = 295$ K and $-22\,000$ deg cm^{-1} at $T = 4.2$ K for low gallium contents. These values are in agreement with data reported for polycrystalline garnets of this composition.[11] The influence of the gallium is not very prominent but a rough extrapolation to zero gallium content leads to $\Delta\theta_F/x \approx 20\,000$ at $T = 295$ K.

The temperature dependence of θ_F is represented in Figs. 11 (a) and 11(b). Both cases lead to a good description of the measured data. The small lead content is taken into account according to the result described before. For $C(T,x)$ in case (II) it turns out that the temperature variation of pure $Gd_3Fe_5O_{12}$ can be used. From case (I) also a bismuth independent dodecahedral coefficient is deduced. For the high Bi contents (samples 8–10) both cases give an approximately identical fit and therefore only the solid lines are shown in Fig. 11(b). The tetrahedral and octahedral magneto-optical coefficients extracted from the fit of case (II) are plotted in Fig. 9 for the samples with the low gallium content. The coefficients from case (I) exhibited a much larger scatter and thus the results have been omitted in Fig. 9. All electric dipole transition coefficients are summarized in Table IV. The linear change of the coefficients with the Bi content is a consequence of the linear increase of θ_F and the fact that the Bi substitution only

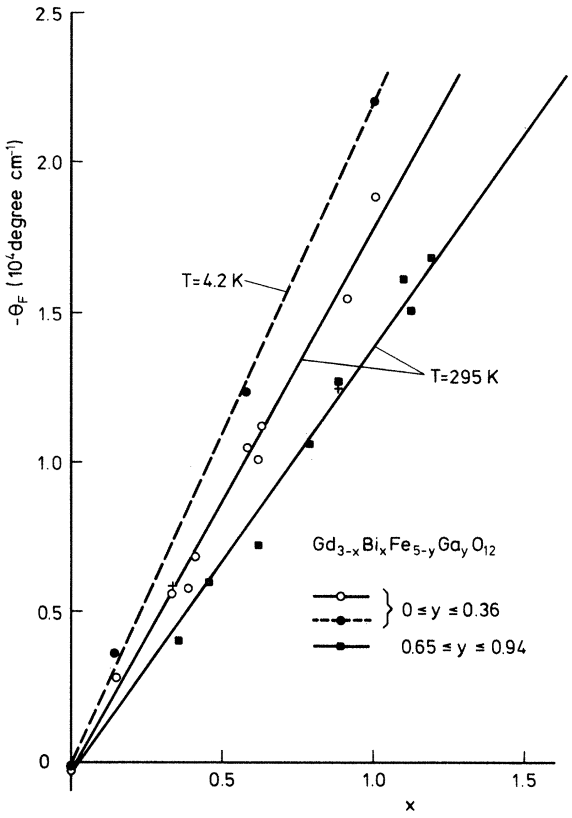

FIG. 10. Concentration dependence of the Faraday rotation at $\lambda = 633$ nm of gadolinium-bismuth iron-gallium garnet films for low and high gallium content. The symbols marked with a cross indicate samples containing a small amount of praseodymium (†) and aluminum (+).

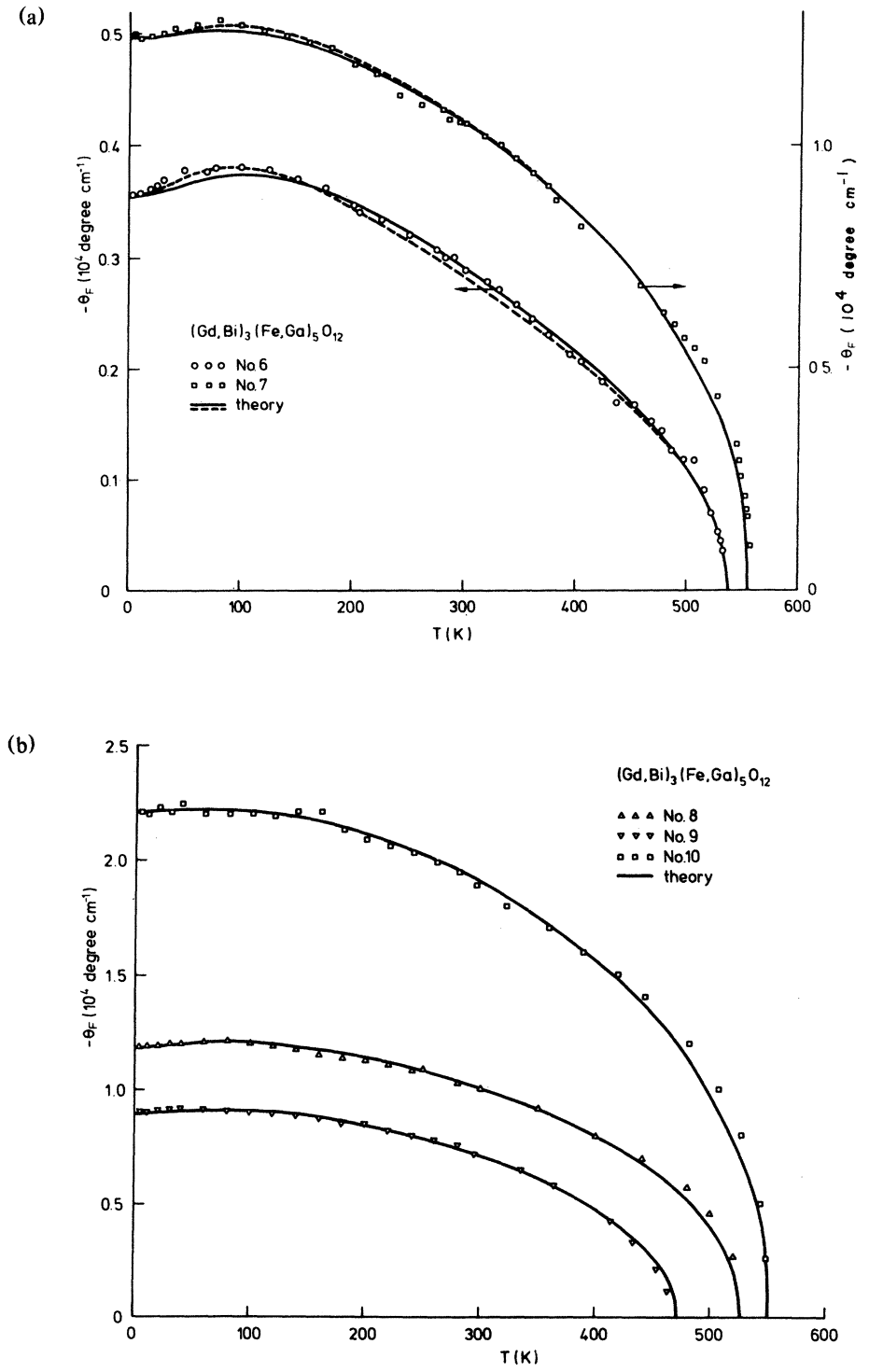

FIG. 11. (a),(b) Temperature dependence of the Faraday rotation for gadolinium-bismuth iron-gallium garnet films at $\lambda = 633$ nm. The theoretical curves have been calculated from Eq. (3) for temperature independent coefficients at *a* (octahedral), *d* (tetrahedral), and *c* (dodecahedral) sites (dashed lines) and temperature-independent coefficients at *a* and *d* sites but *a* temperature-dependent coefficient at the *c* site (solid lines). For the samples with higher bismuth concentrations (b) these two approaches led to identical fits within the limits of these drawings.

affects the dodecahedral sublattice magnetization. The slope, however, is a measure of the strong influence of the bismuth on the iron pair transitions and it is obvious that both iron sites are involved and that for high bismuth concentrations both lattice sites give a negative contribution to θ_F. The good description of the temperature dependence with temperature-independent coefficients on tetrahedral and octahedral sites is reflected in the linear variation of M_a/θ_F^0 vs M_d/θ_F^0 displayed in Fig. 7 where $\theta_F^0 = \theta_F - \Delta\theta_F(\mathrm{Pb}) - CM_c$ is the rotation of the iron sublattices. $\Delta\theta_F(\mathrm{Pb})$ represents the contribution of the lead (see Table I) to the rotation. This linear relationship also holds for the other bismuth-substituted samples investigated.

To account for the small effect of the gallium, two films of composition $Y_3Fe_{5-y}Ga_yO_{12}$ were measured resulting in a linear increase of θ_F as shown in Fig. 12. For comparison the variation at $\lambda = 1150$ nm is given[30,31] where θ_F decreases at $T = 295$ K. For gallium substitutions $y > 1$ an increasing deviation from linearity is expected owing to the reduction of the Curie temperature which for $y = 1.76$ is at room temperature. The magneto-optical coefficients are determined from these data and the calculated sublattice magnetizations[25] using a gallium distribution being present for an equilibrium temperature at $T_e = 1100$ K as shown in Fig. 4 and assuming an equivalent behavior of gallium in $Y_3Fe_5O_{12}$ and $Gd_3Fe_5O_{12}$. The change ΔA and ΔD of the magneto-optical coefficients induced on tetrahedral and octahedral sites by substitution is shown in Fig. 13. Thereby A and D were decomposed as

$$A(x,y) = A_0 + \Delta A(x) + \Delta A(y) \ ,$$
$$D(x,y) = D_0 + \Delta D(x) + \Delta D(y) \ , \tag{7}$$

assuming that the influence of the gallium (y) on the bismuth (x) contribution can be neglected. For small gallium contents the influence is small, but approaching the compositional compensation point of the magnetization the coefficients pass a singularity. This generally holds for all properties being a linear combination of the sublattice magnetizations.[32] This behavior explains the large values of the coefficients

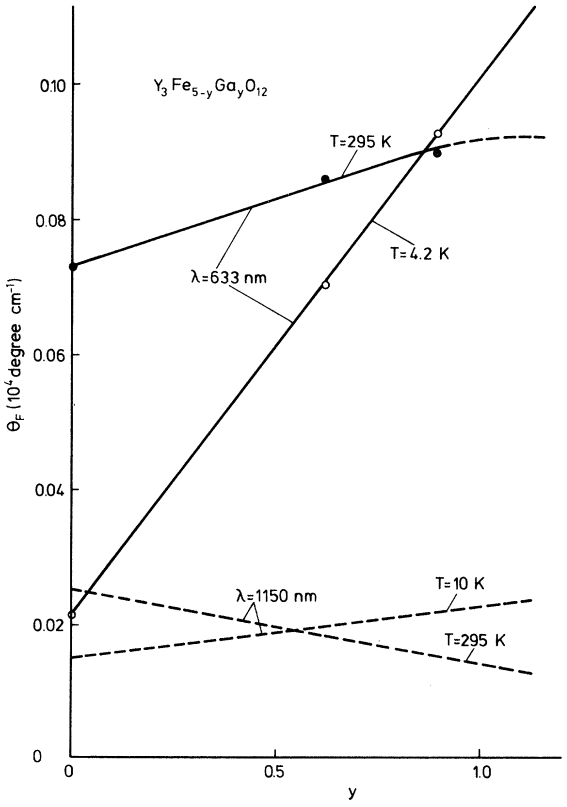

FIG. 12. Concentration dependence of the Faraday rotation of yttrium iron-gallium garnets at $\lambda = 633$ nm (this work) and $\lambda = 1150$ nm (Refs. 30 and 31).

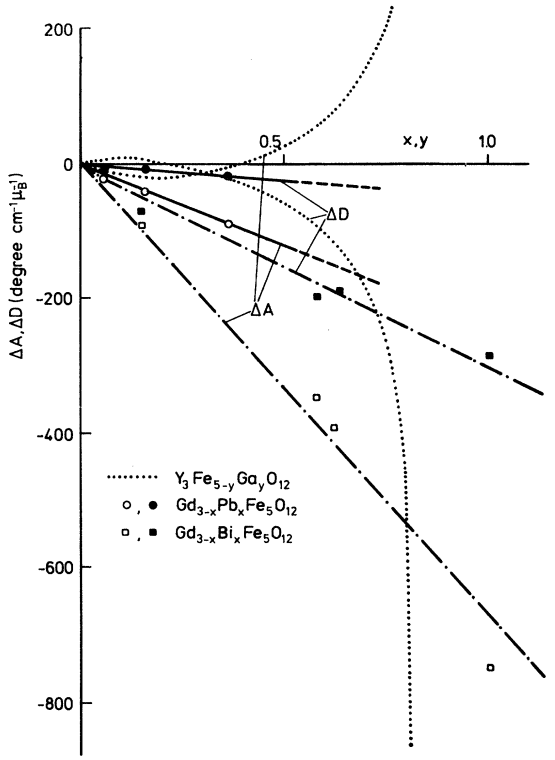

FIG. 13. Variation of the change of the magneto-optical coefficients $\Delta A(x)$, $\Delta A(y)$ and $\Delta D(x)$, $\Delta D(y)$ of yttrium iron-gallium garnets and lead- and bismuth-substituted gadolinium iron garnets. The strong increase of $\Delta A(y)$ and $\Delta D(y)$ of the yttrium iron-gallium garnets has to be attributed to the compositional compensation of the iron sublattices magnetizations.

obtained for sample 9. In this case the amount of gallium is just in the range of the strong increase of $\Delta A(y)$ and $\Delta D(y)$.

The coefficients of the bismuth-substituted films from case (II) were corrected for the gallium contribution and the change $\Delta A(x)$ and $\Delta D(x)$ now depending only on the Bi content are plotted in Fig. 13. In spite of this correction there are still some deviations from the expected linearity. This may be caused by the large influence of small errors of the measured Faraday rotation and the calculated sublattice magnetizations on the evaluation of the coefficients. For the high bismuth substitutions an error of 1% at the temperatures used to fit the theory causes a change in the coefficients of about $50-100\mu_B^{-1}$ deg cm^{-1}. Therefore, a much higher precision of the measured data would be necessary to obtain a significantly improved accuracy of the magneto-optical coefficients.

The accuracy of the electrical dipole transition coefficients given in Table IV, therefore, is much less than indicated by the numbers. In spite of this fact they are tabulated with this accuracy to offer the possibility for recalculating and interpolating the theoretical curves.

IV. DISCUSSION

The incorporation of lead into garnets gives rise to an enhancement of the iron pair transitions and to additional optical transitions for wavelengths below 560 nm (Ref. 3) which cause the increase of the optical absorption and the Faraday rotation via the rise of the superexchange interaction. For the bismuth the large specific rotation can also be attributed to the affected iron pair transitions and again by the increased superexchange interaction.[1,11,29,33,34] Thus a similar mechanism is responsible for the observed rotation of both ions. This is confirmed by the wavelength dependence of θ_F and the angle $\psi_F = \arctan\epsilon_F$ corresponding to the Faraday ellipticity ϵ_F as shown in Fig. 14. The shape of these spectra, in particular for ψ_F, is very similar in this wavelength range except for the absolute magnitudes. For lead-substituted gadolinium iron garnets ψ_F peaks at $\lambda = 488$ nm as compared to gadolinium-bismuth iron garnets where this appears at about $\lambda \approx 450$ nm and for yttrium-bismuth iron garnet at $\lambda \approx 460$ nm.[2] This shift of about 40 nm is also present for the Faraday rotation spectra in the range of wavelengths investigated. This becomes more evident if one considers the change $\Delta\theta_F$ of the rotation induced by the lead substitution (dotted line) which exhibits a shallow minimum in correspondence to the bismuth case and is shifted by the same amount. However, in spite of the isoelectronic configuration of Pb^{2+} and Bi^{3+} it is not necessary that the magneto-optical behavior of these ions is identical owing to the different optical transitions caused by

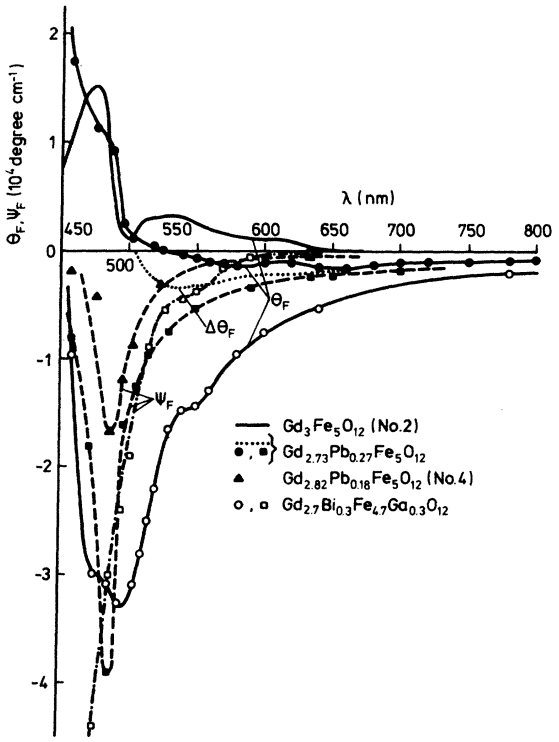

FIG. 14. Wavelength dependence of the Faraday rotation θ_F and the angle $\psi_F = \arctan\epsilon_F$ corresponding to the Faraday ellipticity ϵ_F of lead- and bismuth-substituted gadolinium iron garnets at $T = 295$ K. The dotted line represents the change $\Delta\theta_F$ induced by the lead substitution.

Pb^{2+} and the charge compensating ions as Fe^{2+} and Pb^{4+}.[3] This different behavior indeed is reflected in the different optical absorption spectra.[3,29] In addition, it should be pointed out that the linear variation of θ_F with the total lead content gives an estimate of the lead contribution but a correct assignment to the particular valence state is not yet possible since the matrix elements determining the magneto-optical properties are not available. However, the study of the systems $Gd_{3-x}Pb_xFe_{5-y}M_yO_{12}$ with $M = Sn^{4+}, Ge^{4+}$ suggests that the observed magneto-optical effects essentially are caused by the divalent lead ions.[35]

The analysis of the temperature variation of the Faraday rotation in terms of the sublattice magnetizations showed that a good description of the experimental data is obtained with temperature independent magneto-optical coefficients for a and d sites as demonstrated by Fig. 7. A temperature-dependent dodecahedral coefficient [case (II)] leads to a better fit of the theory to the experimental data than a temperature-independent coefficient [case (I)] as shown by Figs. 6, 11(a), and 11(b) and to more consistency with respect to the dependence on the lead and bismuth content. This supports the results obtained for other rare-earth iron garnets where a

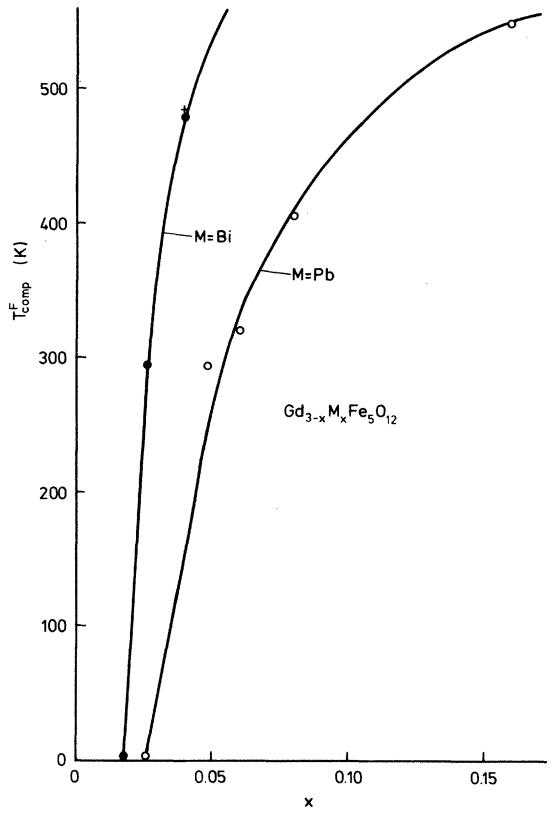

FIG. 15. Concentration dependence of the compensation temperature T^F_{comp} of the Faraday rotation θ_F at $\lambda = 633$ nm and $T = 295$ K of lead- and bismuth-substituted gadolinium iron garnets. The symbol marked with the cross has been calculated where the magneto-optical coefficients were obtained from Fig. 9 by interpolation. The points at $T = 4.2$ and 295 K were taken from Figs. 1 and 10.

strong temperature variation of the dodecahedral coefficient was found.[15] However, the small absolute values of C together with the limited accuracy available for the present experimental data prevent a clear decision in favor of one of these two possibilities. From this point of view the accuracy of the θ_F measurements has to be improved by at least one order of magnitude.

The tetrahedral and octahedral magneto-optical coefficients have opposite signs for the pure garnets. The negative tetrahedral coefficient increases in magnitude while the octahedral drops with a higher slope as discussed in Fig. 13. In particular, for bismuth a sign change of this coefficient occurs at $x_0 \approx 0.74$ thus leading to the strong increase of the negative specific rotation. For a certain substitution and temperature the rotation becomes zero as shown in Fig. 6 for sample 3. For this sample the compensation temperature T^F_{comp} of θ_F occurs at 320 K while the compensation temperature of the saturation magnetization appears at $T_{comp} = 259$ K. The compensation temperature of θ_F is plotted in Fig. 15 as a function of the Pb and Bi content exhibiting a very strong variation as compared to that of the compensation temperature of M_s (see Fig. 1).

This compensation temperature and more generally the concentration and temperature dependence of θ_F of lead- and bismuth-substituted gadolinium iron garnets at $\lambda = 633$ nm can be calculated by extrapolation of the extracted coefficients which are given in Table IV and Figs. 9 and 13. Thus a good estimate of the magneto-optic behavior of these systems can be obtained.

V. CONCLUSIONS

The incorporation of lead and bismuth in gadolinium iron garnets gives rise to a strong negative contribution to the Faraday rotation θ_F for $\lambda \gtrsim 500$ nm where the magnitude of θ_F strongly depends on the wavelength and temperature. For both ions $|\theta_F|$ increases linearly with concentration. The wavelength dependence of θ_F is very similar for Pb- and Bi-substituted garnets although for Pb additional optical transitions presumably are involved. The measured Faraday ellipticity indicates a shift of the spectra for the lead-substituted garnets towards larger wavelengths.

The magneto-optical coefficients deduced from the temperature dependence of the Faraday rotation at $\lambda = 633$ nm and the sublattice magnetizations are temperature independent for a and d sites but for the c sites the experimental data indicate a temperature dependence. The coefficients at a and d sites decrease with increasing Pb and Bi content where in both cases the octahedral coefficient is much more affected. Thus for these ions the iron transitions of both lattice sites are involved and the large magneto-optical effects can be attributed to the pronounced increase of the superexchange interaction.

ACKNOWLEDGMENTS

The authors would like to thank G. Bartels, I. Bartels, and W. Tolksdorf for the growth and preparation of the garnet films, P. Willich for the chemical analysis, and J. Schuldt and M. Rosenkranz for technical assistance.

[1]G. B. Scott and D. E. Lacklison, IEEE Trans. Magn. 12, 292 (1976).
[2]S. Wittekoek, T. J. A. Popma, J. M. Robertson, and P. F. Bongers, Phys. Rev. B 12, 2777 (1975).
[3]G. B. Scott and J. L. Page, J. Appl. Phys. 48, 1342 (1977).
[4]A recent survey of the magneto-optics of garnets is given by J. Dillon, in *Physis of Magnetic Garnets,* edited by A. Paoletti (North-Holland, New York, 1978), p. 379.
[5]Most data on magneto-optics up to 1977 are compiled by P. Hansen, K. Enke, and G. Winkler, in Landolt-Börnstein: *Numerical Data and Functional Relationships in Science and Technology, Part: Iron Garnets,* edited by K.-H. Hellwege (Springer, Berlin, 1977), Series 12a, p. 167.
[6]B. Hill and K. P. Schmidt, Philips J. Res. 33, 211 (1978).
[7]B. Hill and K. P. Schmidt, SID J. 10, 80 (1979).
[8]W. A. Crossley, R. W. Cooper, J. L. Page, and R. P. van Stapele, Phys. Rev. 181, 896 (1969).
[9]G. Abulafya and H. LeGall, Solid State Commun. 11, 629 (1972).
[10]H. Takeuchi, Jpn. J. Appl. Phys. 13, 2059 (1974).
[11]H. Takeuchi, Jpn. J. Appl. Phys. 14, 1903 (1975).
[12]E. V. Berdennikova and R. V. Pisarev, Sov. Phys. Solid State 18, 45 (1976) [Fiz. Tverd. Tela 18, 81 (1976)].
[13]R. Krishnan, T. K. Vien, J. C. Canit, and S. Visnovsky, IEEE Trans. Magn. 13, 1577 (1977).
[14]H. Toda and Y. Nakagawa, J. Phys. Soc. Jpn. 46, 339 (1979).
[15]M. Guillot, A. Marchand, H. LeGall, P. Feldmann, and J. M. Desvignes, J. Magn. Magn. Mater. 15–18, 835 (1980).
[16]D. Mateika , R. Laurien, and Ch. Rusche, J. Cryst. Growth (in press).
[17]W. Tolksdorf *et al.* (unpublished). The relationship between the growth conditions and the composition of these films are planned to be published in a separate paper.
[18]E. E. Anderson, Phys. Rev. A 134, 1581 (1964).
[19]G. F. Dionne, J. Appl. Phys. 42, 2142 (1971).
[20]S. Geller, H. J. Williams, G. P. Espinosa, R. S. Sherwood, and M. A. Gilleo, Appl. Phys. Lett. 3, 21 (1963).
[21]B. Strocka, P. Holst, and W. Tolksdorf, Philips J. Res. 33, 186 (1978).
[22]R. D. Shannon, Acta Crystallogr. A 32, 751 (1976).
[23]P. Hansen, P. Röschmann, and W. Tolksdorf, J. Appl. Phys. 45, 2728 (1974).
[24]P. Röschmann, J. Phys. Chem. Solids 41, 569 (1980).
[25]P. Röschmann and P. Hansen, J. Appl. Phys. (in press).
[26]N. Y. Gorban and V. A. Odarich, Zh. Priklad. Spektrosk. 23, 1106 (1975).
[27]K. Enke and W. Tolksdorf, Rev. Sci. Instrum. 49, 1625 (1978).
[28]K. Shinagawa, H. Takeuchi, and S. Tanigushi, Jpn. J. Appl. Phys. 12, 466 (1973).
[29]G. B. Scott, D. E. Lacklison, J. L. Page, and J. Hewett, Appl. Phys. 9, 71 (1976).
[30]H. Matthews, S. Singh, and R. C. LeCraw, Appl. Phys. Lett. 7, 165 (1965).
[31]J. P. Coeure, D. Challeton, J. Daval, J. P. Jadot, and J. C. Peuzin, Rev. Phys. Appl. 10, 379 (1975).
[32]P. Hansen, in *Physics of Magnetic Garnets,* edited by A. Paoletti (North-Holland, New York, 1978), p. 56.
[33]S. Wittekoek, T. J. A. Popma, and J. M. Robertson, in *Magnetism and Magnetic Materials—1973 (Boston),* edited by C. D. Graham and J. J. Rhyne, AIP Conf. Proc. No. 18 (AIP, New York, 1973), p. 944.
[34]G. B. Scott, D. E. Lacklison, and J. L. Page, J. Phys. C 8, 519 (1975).
[35]P. Hansen, K. Witter, and W. Tolksdorf, Intermag Conference Digest (in press); IEEE Trans. Magn. (in press).